Wind tunnel flow noise measurements using a random design acoustic array

J. Fischer (1), M. Rowan (2), P. Jacquemin (2), D. Lamos (2)

O. Vargas (2), J. Malcolm (2), A. Skvortsov (2) and C. Doolan (1)

(1) School of Mechanical and Manufacturing Engineering, UNSW Sydney, Sydney, Australia
(2) Defence Science and Technology Group, Melbourne, Australia

ABSTRACT

This paper will describe a new aeroacoustic test facility established at the Defence Science and Technology Group (Low Speed Wind Tunnel) in Melbourne. The new test capability utilises a custom 64 microphone acoustic array whose design was optimised for large models. Measurements were carried out on an aeroacoustic model for two flow speeds and for a wide range of pitch and yaw angles. The data were processed using a frequency domain beamforming algorithm assuming monopole sources on the scanning plane. Different noise sources were identified on various parts of the model, notably around the fin and tail regions. Most of the sources were found at mid-frequencies for the lowest flow speed and high frequencies for the highest flow speed. The paper will describe the array design, its implementation as well as the wind tunnel test program.

1 INTRODUCTION

Flow noise is one of the major sources of radiated noise of underwater vehicles and remains one of the main challenges for submarines. Flow noise is very difficult to study experimentally, as it is often masked by other noises, preventing its reliable identification and estimation. Examples include noise of flow control devices (nozzles, valves, discharge vents, etc.), vibration of supporting structures and fan noise. These factors often make any experimental study of flow noise a challenging and often expensive undertaking, especially when working with water or cavitation tunnels (Doolan, 2013; Doolan, 2014).

In the present paper, we present results of an experimental study on an aeroacoustic model conducted in a new aeroacoustic test facility at DSTG. An acoustic array of microphones with a random pattern was employed and the data were processed using the Conventional Beamforming (CBF) and Clean-SC algorithms. Sound pressure level maps were produced to allow identification of the regions of intensive flow noise.

2 BEAMFORMING METHODOLOGY

Beamforming is a common tool used in aeroacoustic testing to locate sound sources. The sound of a source is recorded using a set of microphones, called an acoustic array, usually placed in a two-dimensional plane. The array electronically steers the microphone signals to several positions in a focusing plane where the source is sought. In the time-domain, this process is achieved by delaying each microphone signal regarding to its position and of the focusing point location (Fischer, 2014; Fischer, 2016). This section will summarize the main equations of CBF and of the deconvolution algorithm Clean-SC. For more details, please refer to (Mueller, 2002; Raman, 2013; Sijtsma, 2007).

2.1 Conventional Beamforming

An acoustic array composed of M microphones where the mth microphone is located at $\mathbf{x_m}$ is used to measure the sound of a given source. Each microphone provides a signal that is projected in the frequency domain using a Fourier transform. The Cross-Spectral Matrix (CSM) of the frequency vectors $\mathbf{P}(f) = [p_1,...,p_M]^T$ is constructed using the following convention:

$$\mathbf{C}(f) = \overline{\mathbf{P}(f)\mathbf{P}(f)^H} \tag{1}$$

where superscript ^{H} represents the hermitian transpose and the superscript $\overline{X}$ denotes the averaging of the quantity X in a number of discrete time blocks using Welch's periodogram. All the data presented in this work have been measured with a sampling frequency f_s = 65,536 Hz over a duration T = 32 s. The block-averaging procedure was

performed over 512 blocks of 8192 FFT points (frequency resolution of 8 Hz) with an overlap of 4096 points and using a Hanning window function.

The algorithm then steers the array signals on several positions in a so-called focusing plane where the source is sought. The result is called beamformer output and takes the following expression:

$$Z(\mathbf{y_n}, f) = \frac{\mathbf{h}(\mathbf{y_n}, f)^H \mathbf{C}(f)\mathbf{h}(\mathbf{y_n}, f)}{M(M-1)}, \tag{2}$$

where $\mathbf{h}(\mathbf{y_n}, f) = h(\mathbf{x_m}, \mathbf{x_s}, f)$ is called the steering vector and represents the normalized Green's function between the microphone located at $\mathbf{x_m}$ and the focusing point at $\mathbf{y_n}$. In order to reduce the uncorrelated noise on the microphones, the diagonal elements of the CSM are set to 0; this improves the resolution on the beamforming map (Oerlemans, 2007). The expression of the steering vector is the following:

$$h(\mathbf{x_m}, \mathbf{y_n}, f) = \frac{g(\mathbf{x_m}, \mathbf{y_n}, f)}{|g(\mathbf{x_m}, \mathbf{y_n}, f)|}, \tag{3}$$

where the symbol |.| stands for the absolute value. In CBF, it is assumed that the acoustic sources are monopolar, so the steering vector uses the free-field Green's function for a monopole:

$$g(\mathbf{x_m}, \mathbf{y_n}, f) = \frac{\exp(-jk||\mathbf{x_m} - \mathbf{y_n}||)}{4\pi||\mathbf{x_m} - \mathbf{y_n}||}, \tag{4}$$

where $k = 2\pi f/c_0$ denotes the wavenumber at frequency f in a medium which speed of sound is denoted by c_0 and the symbol $||.||$ stands for the 2-norm.

2.2 Deconvolution using Clean-SC

Clean-SC (Sijtsma, 2007) is an efficient method to remove side lobes on beamforming maps. As it is a deconvolution algorithm, it also provides a constant resolution of the main lobe for all frequencies on the acoustic maps. The algorithm first searches for the position of the maximum in the BF map (called here a 'dirty map'). Once the main lobe has been found, a scaled Point Spread Function (PSF) is created and removed from the dirty map. The PSF is then replaced with a clean beam, i.e. a beam without side lobes, and the process can be repeated on the new dirty map. When the process converges, usually after several iterations, the clean beams obtained at each step are summed all-together with the remaining dirty map obtained at the last iteration. Let us denote by $B^{(p)}$ the clean beam at iteration p while $D^{(P)}$ represents the dirty map obtained at the last iteration. The output of the Clean-SC algorithm at frequency f and for a focusing point located at $\mathbf{y_n}$ can be formulated as follows:

$$A(\mathbf{y_n}, f) = D^{(P)}(\mathbf{y_n}, f) + \sum_{p=1}^{P} B^{(p)}(\mathbf{y_n}, f). \tag{5}$$

2.3 Flow effects

In addition, the background noise, i.e. the flow noise with an empty test-section, was recorded and thus could be removed from the actual array measurements (Humphreys, 1998). All the beamforming maps presented in this work were obtained using this process. The refraction of sound due to the flow is then taken into account by using the approximation for low Mach number (M<0.3) (Padois, 2013):

$$x_{\text{shift}} = MH, \tag{6}$$

where x_{shift} represents the shift of the acoustic sources and H stands for the flow thickness between the source and the microphone array.

When performing CBF in a reverberant test-section, image sources due to the walls can appear on the maps and interfere with the main lobe, leading to an incorrect wrong estimation of the source location. Some solutions have been proposed to reduce this effect (Sijtsma, 2003; Fischer, 2016; Fischer 2017) but no correction has been applied in the present case.

3 EXPERIMENTAL SETUP

3.1 Wind tunnel

Array measurements were performed in the low-speed wind tunnel located at the Defence Science and Technology Group (DST). The wind tunnel has a closed return circuit with an octagonal working section 2.74 m wide, 2.13 m high and 2.93 m long. The maximum velocity in the test section is approximately 100 m/s.

3.2 Model

Acoustic array measurements were carried out using the unclassified BB2 generic submarine model, as an example of a large body with multiple sources of flow noise generation. The model has a length $L = 1.9$ m and a diameter $D = 0.3$ m. The fin is a NACA0015 with a rounded tip. Two NACA0012 airfoils are attached on the sides, known as the fin control surfaces. Four control surfaces are attached to the rear section of the model. These control surfaces are also based on the NACA0012 airfoil profile. Figure 1 shows photographs of the model at three different pitch angles installed in the working section of the wind tunnel. The model was mounted on an arm which allows translation and rotation movement within the vertical plane located at the centre of the working section.

Figure 1: Photographs of the model and the 64 microphone array in the wind-tunnel with a zero (a), positive (b) and negative (c) pitch angle.

3.3 Flow conditions

Measurements were performed for two different flow speeds at low Mach numbers. The model was moved at various positive and negative pitch θ and yaw ϕ angles. The yaw angles were obtained by rotating the model of $90°$ around the horizontal strut so that the array was facing the top of the submarine.

3.4 Acoustic array

The array is composed of 64 1/4" GRAS 40PH phase matched microphones (frequency range [50 Hz ; 10 kHz]). They were connected to a PXIe-4499 24 bit simultaneous sample computer. The design of the array was optimised for the purpose of this particular study and is detailed in section 4.

4 ARRAY DESIGN OPTIMISATION

The aim of this section is to propose an optimised array design to locate acoustic sources on the aeroacoustic model in DST Group's low speed wind tunnel. The size of the array panel is 800 mm × 1,600 mm, as shown in Figure 2. A maximum of 128 microphones is considered. The frequency range of interest is [500 Hz; 16 kHz]. The numerical sources are computed numerically and consist of single monopoles radiating white noise and located at several positions around the submarine model. Some array designs are presented first, followed by CBF (Mueller, 2002) and Clean-SC (Sijtsma, 2007) results.

4.1 The effect of changing the microphone locations

A variety of array designs are considered, each using a maximum of 128 microphones. The first design is an Underbrink multi-spiral array (Mueller, 2002) which will be used as a reference. The second array consists of 2 smaller Underbrink arrays located in each 800 mm × 800 mm half of the panel. The last design is a random array composed of 128 microphones. The composition of each array is summarised in Table 1. The array geometries are presented in Figure 2. The grey rectangle stands for the panel where the microphones will be mounted.

Table 1: Array design summary. For array (a) and (b), in $X \times Y$, X designates the number of arms and Y the number of microphones per arm. Also, each Underbrink array includes an extra centre microphone.

Name	Description	Total
(a) Single Underbrink array	One array of 11 × 11 microphones.	122 microphones.
(b) Double Underbrink array	Two arrays of 9 × 7 microphones each.	128 microphones.
(c) Random array	One array of 128 microphones.	128 microphones.

CBF results are presented in the left column of Figure 3 for each array design. Only the third-octave band centred at f = 8 kHz is shown but similar conclusions were obtained for the other frequency bands. In addition to the CBF results, the maps obtained using the Clean-SC deconvolution algorithm are displayed in the right column of Figure 3. The source locations are presented in green circles and the dashed lines denote the panel in which the array was built.

The first observation is that the location is quite similar between each array as the sources on the front, fin and tail are found. However, the first array (a) is not able to separate the sources on the tail while the others can. When comparing arrays (b) and (c), it appears that even though the resolution is almost the same, the double Underbrink array provides slightly higher side lobes than the random array (c). This is particularly clear when looking at the fin and tail.

The Clean-SC results, shown in the right column of Figure 3, provide a better resolution than the CBF images, as the algorithm removes the peaks (or side lobes) that are coherent with the main lobe. The conclusions are quite similar: array (a) is unable to separate the tail sources where the two other arrays can. The conclusion is that the random array design provides the best results in the present case.

### 4.2 The effect of reducing the number of microphones

The number of microphones will now be reduced to 64 and 32 using the random array design. The case of 128 microphones will also be shown and used as the reference case. Again, the maps have been obtained using CBF and the deconvolution algorithm Clean-SC.

Figure 4 shows the beamforming maps with a random array design using 128, 64 and 32 microphones. Results are shown for the third-octave frequency f = 8 kHz. As can be observed, the difference between the 128 and 64 is minor, on both CBF and Clean-SC maps. This means that 64 microphones are enough to locate the sources in the present numerical case. However, when reducing the number of microphones to 32, several side lobes appear, due to the reduced number of sensors.
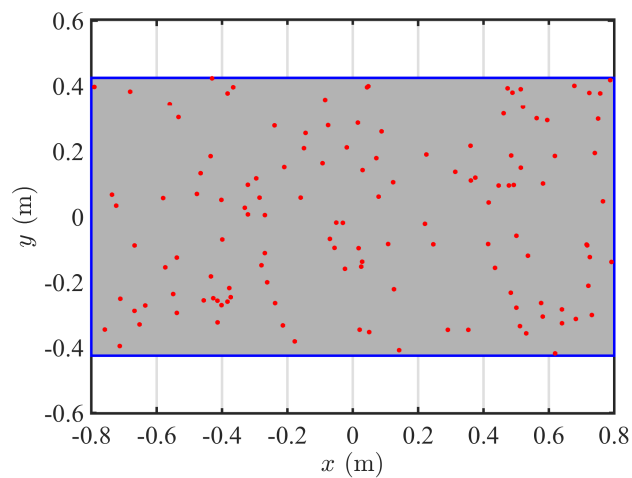
Based on the results presented in this section, it was decided to build an array of 64 microphones with a random design.
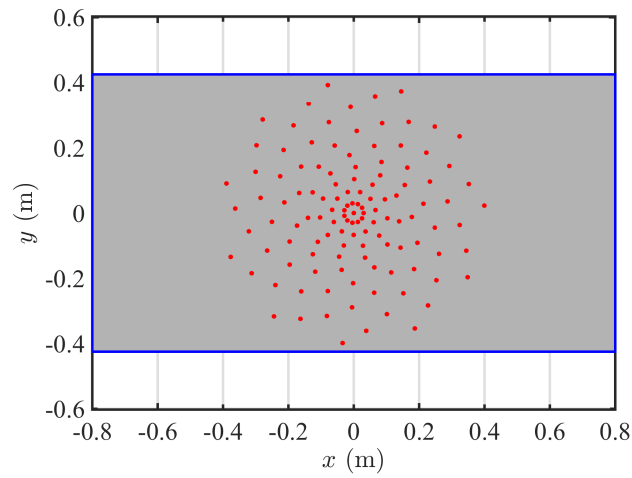
(a)
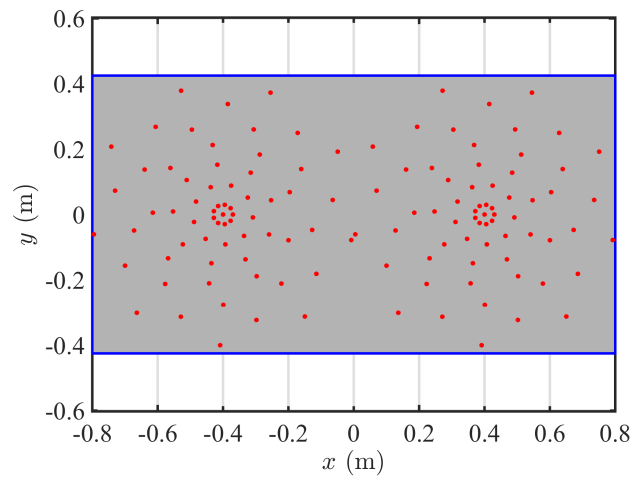
(b)

(c)

Figure 2: (a) Single Underbrink spiral array of 122 microphones, (b) double Underbrink spiral array of 128 microphones and (c) random array of 128 microphones.
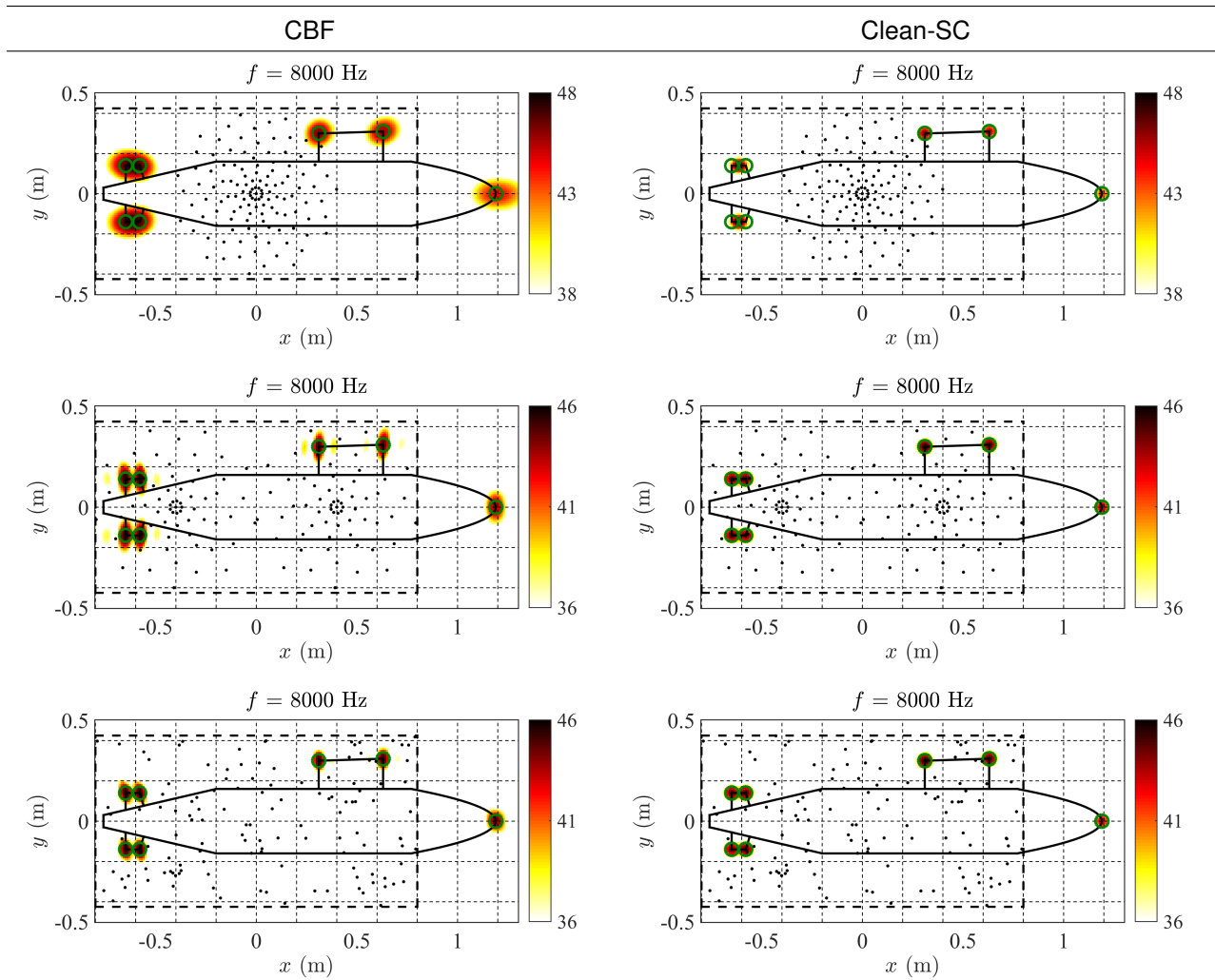
Figure 3: CBF (left) and Clean-SC (right) maps for simulated monopole sources located on the green circles using single Underbrink (first row),double Underbrink (second row) and random (third row) designs at f = 8 kHz.
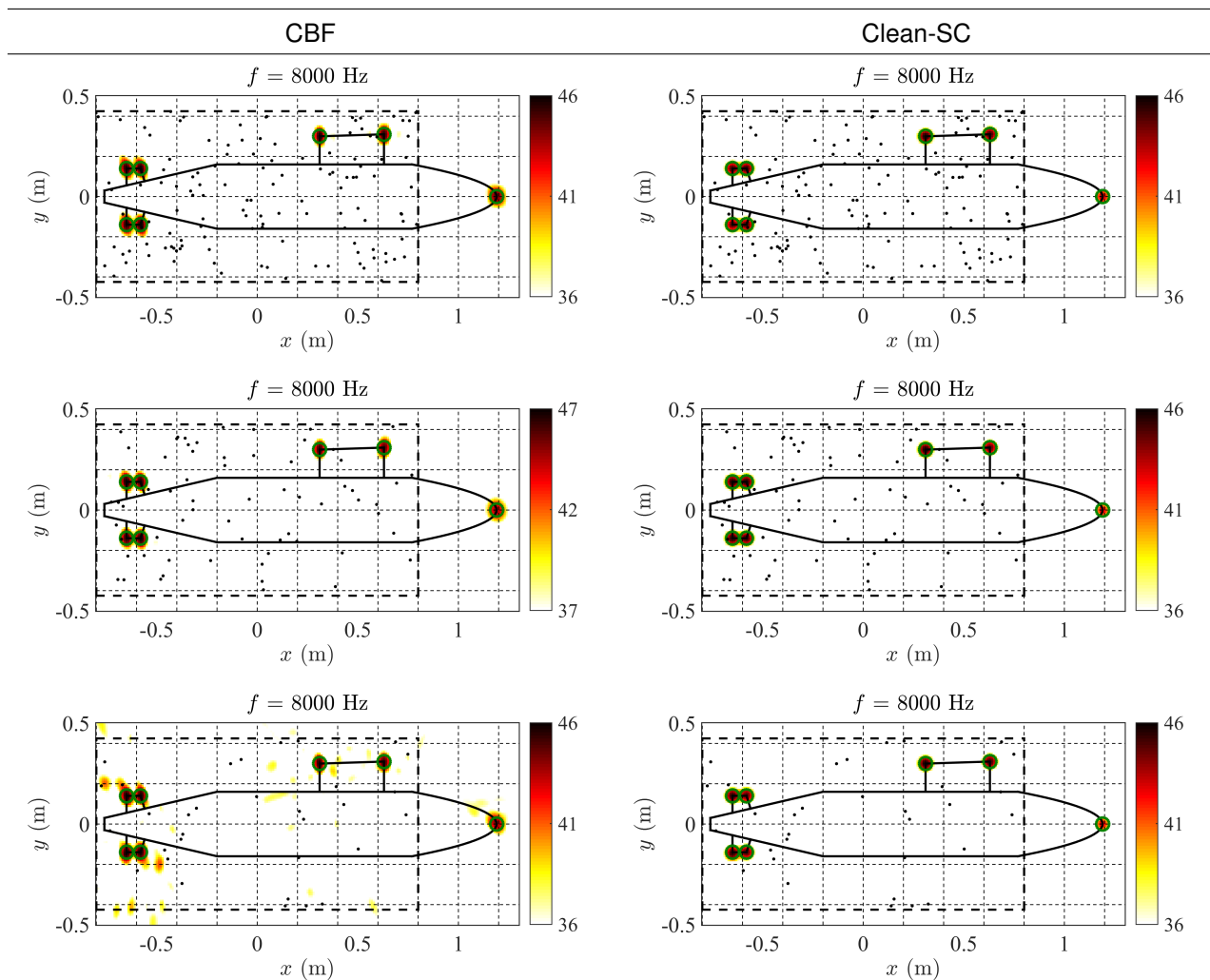
Figure 4: CBF (left) and Clean-SC (right) maps for simulated monopole sources located on the green circles using 128 (first row), 64 (second row) and 32 (third row) microphones at f = 8 kHz.

5 RESULTS

5.1 Single microphone spectra comparison

Figure 5 shows the Power Spectral Density (PSD) of a single microphone located at the centre of the array for a low and high flow speed and for a small and high pitch angle. The solid line corresponds to the model in flow while the dashed one stands for the background measurement (flow with empty test section).

First, Figure 5 (a) corresponds to the model with a small pitch angle and the result is representative to what is observed in a majority of the cases: the noise from the model is the same as the background except at one single frequency and only for the highest flow speed where a peak is observed when the model is present.

For the large pitch angle, several tones are observed at mid frequencies for the lowest flow speed (Figure 5 (b)). This phenomenon is only noticeable for that specific angle and on both the pitch and yaw measurements.
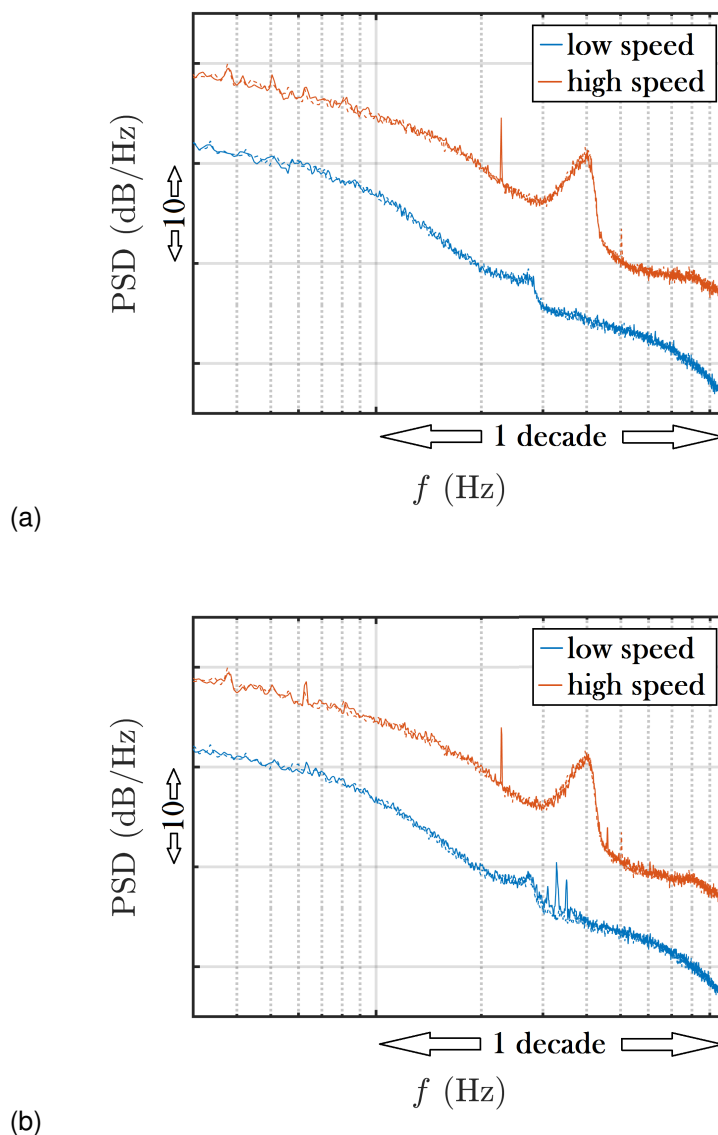

(a)

(b)

Figure 5: PSD of a microphone located at the centre of the array for a low and high flow speed and with a small (a) and large (b) pitch angle.

5.2 Array measurements

Several sources of sound are observed at different locations on the model. Figure 6 shows the example of the the tail noise obtained using CBF (first row) and Clean-SC (second row). The left figures correspond to pitch measurements while the ones on the right are related to the yaw data. Note that all the results presented in

Figure 6 correspond to the lowest flow speed.

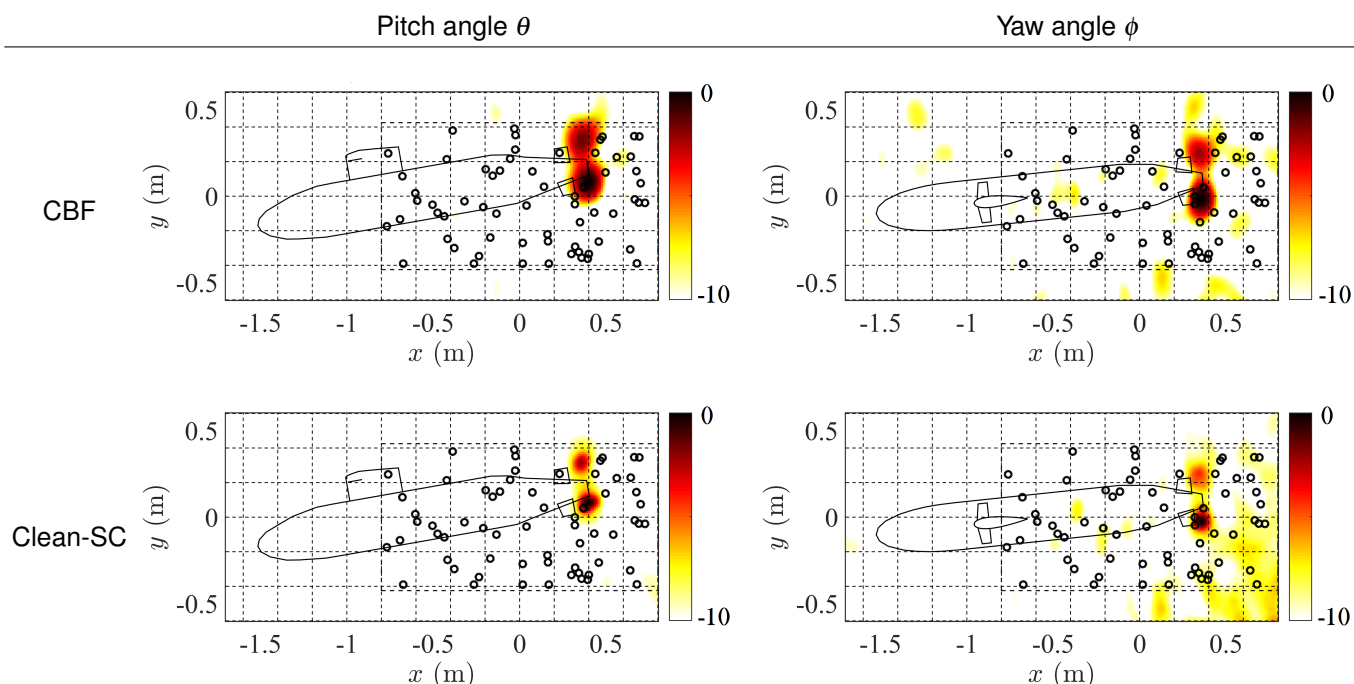| Pitch angle θ | Yaw angle ϕ |

Figure 6: CBF and Clean-SC maps for negative pitch and yaw angles at mid-frequencies for investigating the tail noise.

The beamforming maps from Figure 6 clearly indicate that it is possible to observe the tail noise sources on specific pitch and yaw angles. Also, the maps are quite clean even when using CBF. When using the deconvolution algorithm Clean-SC, the result is very similar, except that the resolution is improved with the latter algorithm.

6 CONCLUSION

A range of acoustic array measurements on the Joubert BB2 generic submarine model were conducted in the DST Group's Low Speed Wind Tunnel. The model was moved over several pitch and yaw angles at two flow speeds. The acoustic array consisted of 64 microphones which were randomly located.

First, the array design was investigated in order to be adapted to the low speed wind tunnel. It was found that the best results on the CBF maps were obtained using a random design with 64 microphones.

Some spectra obtained with and without the model in the tunnel were compared. A tone was present at mid-frequencies in all the spectra obtained with the model at the highest speed. At higher frequencies, some tones were also depicted with the model in flow but only at the lowest speed and for a few angles. The beamforming maps have shown that the tail noise can be accurately found at specific pitch and yaw angles.

In the future, we expect to repeat these experiments using an improved acoustic array and a telescopic sting that improves the accuracy of the alignment of the Joubert BB2 model relative to the microphone array. In addition, acoustic absorption material will be installed to reduce the wind tunnel background noise.

REFERENCES
Doolan, C., Brandner, P., Butler, D., Pearce, B. Moreau, D., and Brooks, L. 2013. 'Hydroacoustic Characterisation of the AMC Cavitation Tunnel'. In *Proceedings of Acoustics*. Victor Harbor, Australia.

Doolan, C, Moreau, D., Brandner, P., Pearce, B., and De Graaf, K. 2014. 'Noise from sub-boundary layer steps'. In *19th Australasian Fluid Mechanics Conference*. Melbourne, Australia.

Fischer J., Valeau, V., and Brizzi, L.-E. 2014. 'Beamforming of aeroacoustic sources in the time domain'. In *Inter-noise*. Melbourne, Australia.

Fischer, J., Valeau, V., and Brizzi, L.E. 2016. 'Beamforming of aeroacoustic sources in the time domain: an investigation of the intermittency of the noise radiated by a forward-facing step'. *Journal of Sound and Vibration* 383: 464–485.

Fischer, J., and Doolan, C. 2016. 'An empirical de-reverberation technique for closed-section wind tunnel beamforming'. In *22nd AIAA/CEAS Aeroacoustics Conference*. Lyon, France.

Fischer, J., and Doolan, C. 2017. 'Beamforming in a reverberant environment using numerical and experimental steering vector formulations'. *Mechanical Systems and Signal Processing* 91: 10–22.

Humphreys, W.M., Brooks, T.F., Hunter, W.M., and Meadows, K.R. 1998. 'Design and use of microphone directional arrays for aeroacoustic measurements'. In *36th Aerospace Sciences Meeting & Exhibit*. Reno, Nevada.

Mueller, T. 2002. *Aeroacoustic measurements*. Springer-Verlag.

Oerlemans, S., Broersma, L., and Sijtsma, P. 2007. 'Quantification of airframe noise using microphone arrays in open and closed wind tunnels'. *International Journal of Aeroacoustics* 6: 309–331.

Padois, T., Prax, C., and Valeau, V. 2013. 'Numerical validation of shear flow corrections for beamforming acoustic source localisation in open wind-tunnels' *Applied Acoustics* 74: 591–601.

Raman, G. Ramachandran, C., Srinivasan, K., and Dougherty, R. 2013. 'Advances in experimental aeroacoustics'. In *International Journal of Aeroacoustics* 12: 579–637.

Sijtsma, P., and Holthusen, H. 2003. 'Corrections for mirror sources in phased array processing techniques'. In *9th AIAA/CEAS Aeroacoustics Conference*. Hilton Head, South Carolin.

Sijtsma, P. 2007. 'CLEAN based on spatial source coherence'. In *13th AIAA/CEAS Aeroacoustics Conference*, Rome, Italy.